Global Environmental Change 61 (2020) 102037

Contents lists available at ScienceDirect

Global Environmental Change

journal homepage: www.elsevier.com/locate/gloenvcha

Hard or soft flood adaptation? Advantages of a hybrid strategy for Shanghai

Shiqiang Du[a,b,*], Paolo Scussolini[b], Philip J. Ward[b], Min Zhang[a], Jiahong Wen[a], Luyang Wang[a], Elco Koks[b], Andres Diaz-Loaiza[b,c], Jun Gao[a], Qian Ke[c], Jeroen C.J.H. Aerts[b,*]

[a] School of Environmental and Geographical Sciences, Shanghai Normal University, Shanghai, China
[b] Institute for Environmental Studies, Vrije Universiteit Amsterdam, Amsterdam, the Netherlands
[c] Department of Hydraulic Engineering, Delft University of Technology, Delft, the Netherlands

ARTICLE INFO

Keywords:
Climate change
Nonstationarity
Coastal flood
Risk management
Cost-benefit analysis

ABSTRACT

Flood risk is expected to increase in coastal cities, particularly in Asian megacities such as Shanghai. This paper presents an integrated modeling framework to simulate changes in the flood risk in Shanghai and provide a cost-benefit analysis of multiple adaptation strategies used to reduce risk. The results show that the potential flood risk will increase dramatically as a result of sea level rise, land subsidence, and socioeconomic development. By 2100, the expected annual damage could reach 0.8% (uncertainty range: 0.4%–1.4%) of local GDP under an optimistic emission scenario (RCP4.5), compared to the current value of 0.03%. All of the adaptation strategies can effectively reduce the flood risk under the current conditions and those in 2050. In contrast to the 'hard' flood protection strategies (i.e., storm-surge barriers and floodwalls), the 'soft' strategies (i.e., building codes and nature-based measures) cannot substantially reduce the flood risk in 2100. However, the soft strategies can play a critical role in reducing the residual risk resulting from the hard strategies. A 'hybrid' strategy combining a storm-surge barrier, wet-proofing, and coastal wetland development outperforms both hard and soft strategies in terms of low residual risk and high benefit/cost ratio. Additionally, the hybrid strategy can also enable a larger reduction in casualties. These findings imply that managing flood risk is more than the use of single adaptation measures. The methodology developed in this paper can enlighten Shanghai and other coastal cities on an economically and socially feasible adaptation strategy in an uncertain future.

1. Introduction

Flooding is one of the most costly natural hazards in terms of economic losses (Najibi and Devineni, 2018; Wallemacq et al., 2018). Both flood frequency and consequences are expected to increase in the future as a result of climate change and socioeconomic development (Willner et al., 2018; Winsemius et al., 2016). Specifically, the flood hazard of coastal cities is projected to increase as a result of various factors, including sea level rise (SLR), land subsidence, a potential increase in the probability and intensity of storm surges, and an increase in peak discharge in rivers flowing into coastal zones (Lin et al., 2016; Wahl et al., 2017). Moreover, many cities, particularly those in Asia, will experience increasing flood exposure due to rapid urbanization (Du et al., 2019; Ehrlich et al., 2018). Therefore, it is important to investigate how flood risk will change in the future and how cities can effectively and efficiently adapt to dynamic risk challenges (Aerts et al., 2014; Hinkel et al., 2018; Jongman, 2018).

Several studies have examined how flood adaptation measures can cause changes in flood risk in coastal megacities under the assumptions of various long-term risk projections and flood adaptation scenarios. For example, studies for Ho Chi Minh City, Vietnam (Lasage et al., 2014; Scussolini et al., 2017), and Jakarta, Indonesia (Ward et al., 2011b), have focused on how SLR affects the exposure of people and assets. These studies have explored various adaptation options, including measures at the household level. A major study of the city of London and the greater Thames Estuary assessed adaptation strategies and adaptation tipping points assuming multiple SLR scenarios, including an extreme scenario of +2.7 m during 2010–2100 (Environment Agency, 2012). Studies on New York City and Los Angeles have conducted cost-benefit analyses to estimate the economic feasibility of using dikes and storm-surge barriers to reduce hazards and spatial planning measures to reduce exposure and vulnerability (Aerts et al., 2014; de Ruig et al., 2019). In addition, several regional-scale studies in riverine floodplains have assessed urban flood risk and adaptation in Tyrol, Austria (e.g., Thieken et al., 2016), and have simulated the economic performance of household-level adaptation measures in the Elbe and Danube catchments in Germany (e.g., Kreibich et al., 2011). Studies on flood risk adaptation are still rare for

* Corresponding author.
E-mail addresses: shiqiangdu@shnu.edu.cn (S. Du), jeroen.aerts@vu.nl (J.C.J.H. Aerts).

https://doi.org/10.1016/j.gloenvcha.2020.102037
Received 18 June 2019; Received in revised form 29 December 2019; Accepted 20 January 2020

Asian coastal cities, even though recent global studies have shown that urban flood risk in Asian cities is increasing more rapidly than that in other flood-prone cities (Hallegatte et al., 2013; Winsemius et al., 2016).

Shanghai, China's biggest city and a global financial hub, is one of the megacities most at risk from coastal flooding globally (Balica et al., 2012). According to the results of the global study by Hallegatte et al. (2013), Shanghai may face the largest increase in flood risk worldwide as a result of climate change and socioeconomic development. Existing research has examined the flood hazard dynamics of Shanghai using hydrodynamic models. For example, Wang et al. (2012) simulated how the flooding associated with Typhoon Winnie (1997) could hypothetically change in the future using a linear extrapolation of land subsidence and SLR in the future and the hydrodynamic MIKE 1 D/2 D model, without considering the probabilities of the flood events. Yin et al. (2015) applied the 2 D hydrodynamic FloodMap model to simulate future changes in flood extent and depth under the influences of land subsidence, SLR and urban expansion, but this study was limited to only the area of Shanghai along the banks of the Huangpu River. Ke (2014) simulated flood extents and depths associated with different storm surge return periods but did not consider the future.

A quantification of the socioeconomic impacts of flooding in Shanghai has not yet been carried out, nor has there been an assessment of the costs and benefits of adaptation strategies used to reduce future risk. To address this issue, this paper aims to (1) assess the flood risk in Shanghai under future projections of SLR, land subsidence, and socioeconomic development and (2) analyze the costs and benefits of several adaptation strategies used to reduce flood risk. To achieve this, an integrated modeling framework that extends the spatial domain of previous studies to encompass both oceanographic and terrestrial hydrodynamic modeling is developed; this model incorporates scenario analysis, risk analysis and a cost-benefit analysis of adaptation measures.

2. Case study: Shanghai

Shanghai is the largest metropolis in China. In 2015, Shanghai housed 1.8% (or 24.2 million) of China's total population and produced 3.7% (US$ 403.4 billion) of the national gross domestic product (GDP). The city is prone to flooding because of its low-lying coastal geography, and 85.3% of the territory is prone to both astronomical high tides and a frequent occurrence of storm surges (Du et al., 2015; Wang et al., 2012). The situation has worsened as Shanghai's territory expanded by 9.3%, or 587 km^2, through coastal land reclamation between 1987 and 2017 (Sengupta et al., 2018). One of the deadliest storm-surge events killed more than 29000 people in Shanghai in 1905; Typhoon Winnie killed seven people and flooded more than 5000 households in 1997 (Wen, 2006). An extended list of historical floods in Shanghai is available in supplementary *Table S1*.

For flood management, Shanghai currently relies on 'hard' flood defenses, such as sea dikes and river floodwalls (Du et al., 2015) (*Fig. 1a*). Depending on the location, the sea dikes are designed against 100- or 200-year flood water levels, which are based on extreme water-level data collected in 1984. The floodwalls along the Huangpu River (which is under tidal influence) are designed against a 1000-year storm surge in the central city and against a 50-year flood in the upstream areas (Wang et al., 2012) (a detailed map of the sea dikes and floodwalls is available in supplementary *Figure S1*). Shanghai is likely one of the best protected Chinese cities despite the use of older data; however, SLR and land subsidence have lowered the protection levels of the defense structures since their implementation (Xian et al., 2018).

3. Data and methods

We adopt a modeling framework that integrates hydrodynamic modeling, flood risk analysis, future scenarios, and adaptation strategies (i.e., combinations of specific adaptation measures) to assess the flood risk dynamics and the effects of adaptation strategies on reducing risk (*Fig. 2*).

3.1. Hydrodynamic modeling

Hydrodynamic modeling is conducted to produce flood hazard maps associated with the storm surges of four return periods, namely, 200, 500, 1000, and 5000 years (supplementary *Figure S2*). To simulate oceanographic and terrestrial hydrodynamic processes, we couple the TOMAWAC, TELEMAC, and MIKE 1 D/2 D models. The TELEMAC and the TOMAWAC models are used to simulate the hydrodynamic processes related to tides and waves, respectively, with a temporal resolution of 10 s, based on 43750 flexible triangles. The bathymetry data are derived from a data-survey provided by the Shanghai Municipal Water Authority (SMWA, 2013). Details about TOMAWAC are available in Hervouet (2000), and about TELEMAC in Benoit et al. (1997). The models are calibrated and validated for Shanghai in Zhang et al. (2018). Overall, the models agree with the hourly observed water levels ($R^2 > 0.94, p < 0.01$) and velocities ($R^2 > 0.81, p < 0.01$) during two tidal events.

Next, MIKE 1 D/2 D (DHI MIKE, 2011) is applied to model the propagation of coastal flood waters in river channels and over land surfaces. The spatial resolutions for channels and land surfaces are 1000 m and 60 m, with temporal resolutions of 30 s and 2 s, respectively. The river channels are delineated on the basis of 1-m interval isobathymetric lines of the Huangpu River (Yin et al., 2015). The land surface elevation is generated from a 0.5-m contour map from 2005 (Yin et al., 2015). The current sea-dike and floodwall elevations are derived from SMWA (2013). The rainfall and river discharge data are derived from observations during Typhoon Winnie in August 1997, and these data are superimposed on all coastal flood simulations. The MIKE models are calibrated and validated by Wang et al. (2019): the differences between the observed and simulated water levels were less than 0.10 m in 81% of the 120 data points, and the simulated flood area agrees with the reported data from Typhoon Winnie in 1997.

3.2. Flood risk analysis

Two kinds of flood risk are quantified: expected annual damage (EAD) and expected annual casualties (EAC). The former includes damages to land uses and vehicles, excluding indirect impacts, e.g., impacts on businesses resulting from infrastructural damages. Land-use damages are calculated by combining the flood hazard maps with land-use-based exposure via depth-damage ratios, using an adapted version of the Damage Scanner model (Koks, 2019). The fine-scale land-use map is derived from high-resolution aerial photographs (Shen et al., 2019). The maximum value of each land-use class is estimated based on data from the Shanghai Xinyuan Engineering Cost Consulting Co., Ltd., and the Shanghai Statistical Bureau (2016). The land-use specific depth-damage ratios are adopted from Yin et al. (2012) (supplementary *Figure S3*). Additionally, vehicle losses are evaluated based on the depth-damage ratios from Martínez-Gomariz et al. (2018) (supplementary *Figure S4*). Potential casualties are estimated by combining flood depths and population distribution through a depth-casualty ratio curve (Di Mauro and De Bruijn, 2012; Jonkman et al., 2008; Yin et al., 2012) (supplementary *Figure S5*). The population distribution is disaggregated from Shanghai neighborhood-level census data (Gu et al., 2018). The economic damages and potential casualties are calculated for each of the four return periods (200, 500, 1000, and 5000) and then integrated across their annual exceedance probabilities to yield the values of EAD and EAC (Ward et al., 2011a).

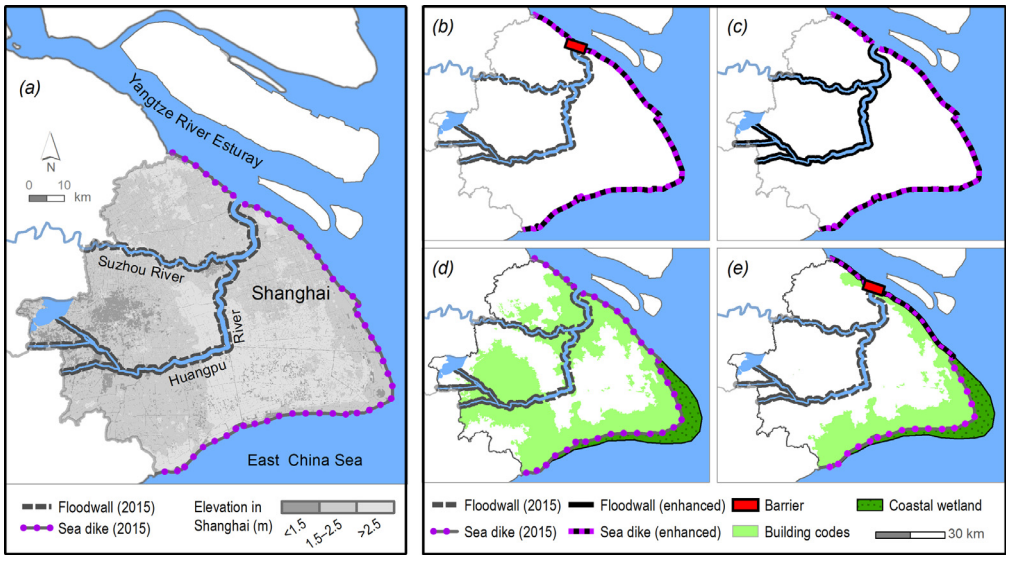

Fig. 1. Mainland Shanghai (in gray; islands are excluded from the study) and its current flood protection (*a*). Also shown are the future adaptation strategies considered in this study: 'hard' protection strategies with a new storm-surge barrier (*b*) and with enhanced floodwalls and sea dikes (*c*); 'soft' strategies that strengthen the building codes and natural coast (*d*; six combinations, see *Table 2*); and a 'hybrid' strategy, which combines elements from the other strategies (*e*).

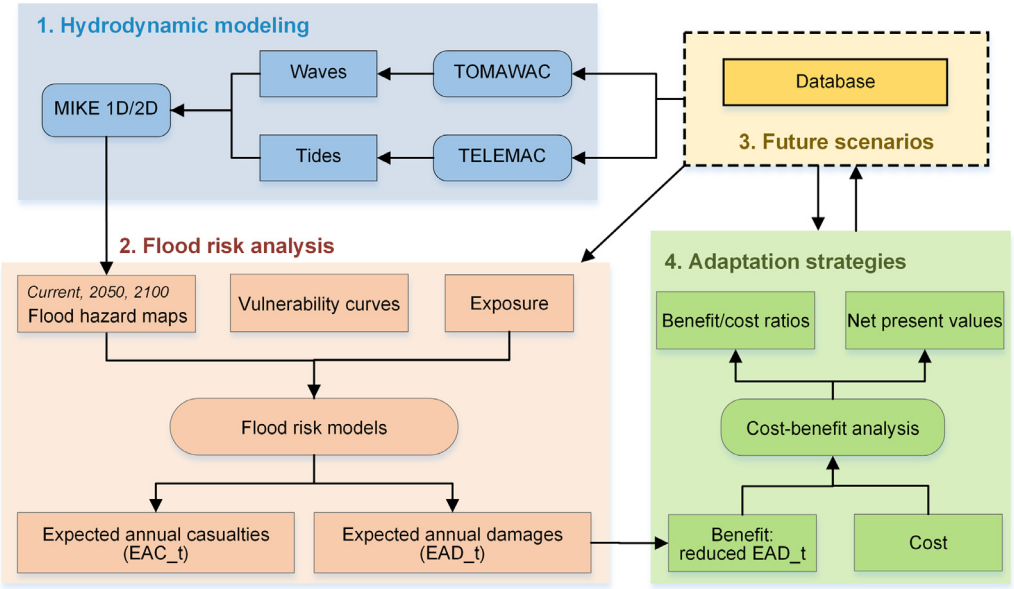

Fig. 2. A framework for assessing the risk and adaptation strategies, encompassing four steps: (1) hydrodynamic modeling, (2) flood risk analysis, (3) future scenarios, and (4) adaptation strategies. Models and processes are represented by rounded boxes, while datasets are represented by squared boxes.

3.3. Future scenarios

We investigate the future flood risk for 2050 and 2100 considering three driving factors: socioeconomic development, SLR, and land subsidence (*Table 1*). Socioeconomic development scenarios are extracted from a gridded regional projection for population (Jiang et al., 2017) and for GDP (Jiang et al., 2018), which are based on the shared socioeconomic pathways (SSPs) (O'Neill et al., 2014). The SSP2 and SSP5 scenarios of future GDP and population are used in this study.

We employ SLR estimates from an ensemble of process-based models (Jevrejeva et al., 2014). The 5%, 50%, and 95% SLR estimates are used for the RCP (representative concentration pathway) 4.5 and RCP8.5 emission scenarios. Additionally, a RCP8.5 high-end scenario is employed as a pessimistic projection from several alternative methods

Table. 1
Future drivers of flood risk in Shanghai (reference year: 2015).

	Current	Year 2050			Year 2100		
		RCP4.5	RCP8.5	RCP8.5 high-end	RCP4.5	RCP8.5	RCP8.5 high-end
SLR (cm)*	0	21 (15–27)	24 (17–31)	28 (17–50)	51 (34–68)	74 (55–98)	87 (49–187)
Land subsidence (cm)	0	18	18	18	43	43	43
Population	2015	SSP2	SSP5	SSP5	SSP2	SSP5	SSP5
GDP	2015	SSP2	SSP5	SSP5	SSP2	SSP5	SSP5

* The median estimates for the future scenarios are shown with the 5% and 95% bounds in the brackets.

Table. 2
Proposed adaptation strategies for Shanghai.

BAU trajectory	Hard strategies	Soft strategies	Hybrid strategy
Business-as-usual	***Barrier***	***Building codes (three sets)***	***Hybrid***
River floodwalls (2015)	Storm-surge barrier	Wet-proofing/	Storm-surge barrier
Sea dikes (2015)	Sea dikes (enhanced)	Dry-proofing/	Wet-proofing (coastal areas)
		Elevation	Sea dikes (north part enhanced)
	Floodwall	***Wetland***	Wetlands (southeast coasts)
	Floodwalls (enhanced)	Building codes (three sets)	
	Sea dikes (enhanced)	Coastal wetlands	

of estimating SLR (Jevrejeva et al., 2014). Finally, we use a land subsidence scenario resulting from propagating the current rate of 5 mm/year (Wang et al., 2012; Xian et al., 2018).

3.4. Adaptation strategies

We consider a business-as-usual (BAU) trajectory and three kinds of adaptation strategies (*Table 2*, *Fig. 1 b–e*). The BAU trajectory does not apply any new adaptation measures and assumes maintenance of the current floodwalls and sea dikes at their current heights. The adaptation strategies are as follows: (1) two 'hard' flood protection strategies; (2) six 'soft' strategies; and (3) one 'hybrid' strategy that combines the hard and soft strategies.

The hard strategies reduce flood risk by changing the flood hazard probability. They include two sets of measures: developing a storm-surge barrier at the mouth of the Huangpu River (barrier, *Fig. 1b*) (Lu, 2007) and, alternatively, upgrading the Huangpu-River floodwalls to a 1000-year level floodwall (*Fig. 1c*). Both the barrier and the floodwall strategies include upgrading the sea dikes to a 200-year protection level, according to Shanghai's master plan for 2017–2035 (Shanghai Municipal People's Government, 2018). The design standards of the storm-surge barrier, floodwall, and sea dike are developed based on a future SLR scenario: the RCP4.5 median estimate in 2100. In comparison, the alternative flood protections are designed under current conditions and are presented only in the Discussion section.

The soft strategies consider two sets of measures (*Fig. 1d*). The building-code strategies enhance building codes for individual properties, including wet-proofing, dry-proofing, and building elevation (Aerts et al., 2014; de Ruig et al., 2019; Scussolini et al., 2017). These measures are effective by reducing the flood depth-damage ratios, although the exact damage reduction rates are uncertain (supplementary *Text S1*). Additionally, the 'wetland' strategies also include coastal wetlands on reclaimed lands from the sea (through sand nourishment), which is similar to the Dongtan Wetland on the east of Shanghai's Chongming Island (supplementary *Figure S1*) (Ma et al., 2004). The wetlands can work as a soft floodwall to protect the sea dikes and reduce impacts of storm surges (supplementary *Text S1*).

The feasibility of these adaptation strategies is presented in supplementary *Tables S2*. For each strategy, we estimate the initial investments and maintenance costs (where applicable) using data from the literature and local knowledge. These results are reported in supplementary *Tables S3*.

3.5. Cost-benefit analysis

The adaptation strategies are economically evaluated through a cost-benefit analysis (Aerts et al., 2014). The cost includes both initial investments and maintenance costs (supplementary *Table S3*). The benefits are expressed as the reduction in EAD from the BAU trajectory. For each strategy, the net present value (NPV), the payoff period, and the benefit/cost ratio are estimated. The NPV provides the amount of net economic benefits that an adaptation strategy generates:

$$\mathrm{NPV} = \sum_{t=0}^{T} \frac{Bt - Ct}{(1+r)^t} \tag{1}$$

where B_t is the benefit (i.e., avoided EAD) of an adaptation strategy in year t; C_t is the cost in year t, including the initial investments and annual maintenance costs; r is the discount rate; and the investment horizon is T years (i.e., the 85-year period from 2015 to 2100). A positive NPV means the sum of the discounted B_t exceeds the sum of the discounted C_t over the T years. Similarly, the payoff period indicates the number of years in which the cumulative B_t exceeds the cumulative C_t.

The benefit/cost ratio represents the economic efficiency in terms of the relative benefits per dollar invested in a strategy:

$$\text{benefit/costratio} = \sum_{t=0}^{T} \frac{Bt}{(1+r)^t} \Big/ \sum_{t=0}^{T} \frac{Ct}{(1+r)^t} \tag{2}$$

If the benefit/cost ratio $>$ 1, then the NPV $>$ 0, the payoff period $<$ T, and the strategy is economically attractive. Both the benefit/cost ratio and the NPV are included in this paper, as they provide different perspectives: the benefit/cost ratio shows the relative benefit per dollar investment of a strategy, while the NPV reveals the total net economic benefit from a strategy. Additionally, the payoff period indicates how long it takes for an adaptation investment to be paid off by the cumulative economic benefits.

3.6. Uncertainty analysis

Uncertainties are addressed in four steps of the modeling framework. First, we employ multiple future scenarios by using RCP-based SLR estimates and SSP-based socioeconomic projections. Second, to further account for future sea-level uncertainty, we use the 5%, 50%, and 95% values of each SLR projection. The multiple SLR scenarios and bounds enable us to include a wide range of uncertainties. Third, we account for the uncertainty in the cost-benefit analysis by using a broad range of discount rate values. The discount rate reflects the opportunity costs of public investments with a long time horizon. It is an uncertain and exogenously determined parameter, involving intense debate in literature on the economics of climate change (Aerts et al., 2014; de Ruig et al., 2019; Scussolini et al., 2017). We thus employ three discount rates: the Chinese official discount rate of 8% (NDRC and MHURD, 2006) as a higher bound, a lower-bound discount rate of 4% following the interbank lending rates in Shanghai to appreciate the long-term benefits of investments, and an in-between rate of 6%. Furthermore, to make our analysis more robust to unquantified sources of uncertainty during modeling, we express the results in terms of the relative changes in flood risk across scenarios rather than in absolute values.

4. Results

4.1. Flood risk dynamics under a business-as-usual trajectory

For the current 200-year flood simulation, 6% (or 330 km^2) of Shanghai is flooded by $\geq$0.25 m of water, mainly in the southeastern coastal areas. However, for a 1000-year flood, the simulated flood area

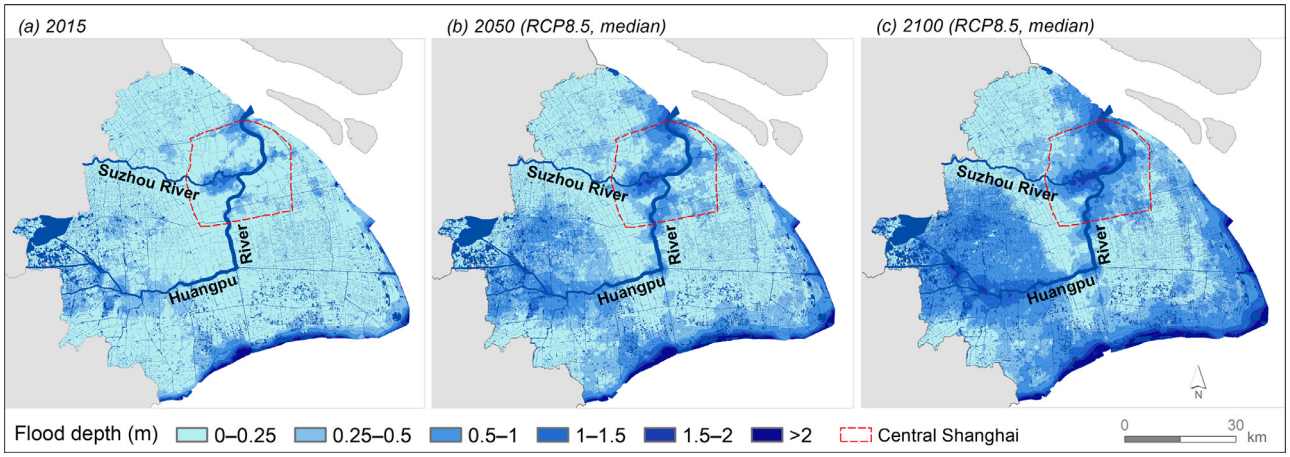

Fig. 3. Flood depths for 1000-year storm surges for current condition (a), 2050 (b) and 2100 (c) in a business-as-usual trajectory.

deeper than 0.25 m reaches 19% (or 1014 km^2) of Shanghai, flooding the urban center significantly (*Fig. 3 a*). With the RCP8.5 scenario of SLR and land subsidence, a 1000-year flood is simulated to inundate 44% (or 2398 km^2, median estimate) of Shanghai with ≥0.25 m water in 2050 (*Fig. 3b*) and 76% (or 4118 km^2) in 2100 (*Fig. 3c*).

Under current conditions, the simulated EAD is US$ 106 million/year (2015 price), accounting for 0.03% of local GDP in 2015. Without adaptation, SLR and land subsidence increase the future EAD dramatically. By 2100, the simulated increase ranges from a factor of 32 (18–54, the numbers in brackets are the 5%–95% bounds on the SLR projections; same hereafter) under the RCP4.5 scenario to a factor of 92 (30–340) under the RCP8.5 high-end scenario. Moreover, socio-economic growth increases the EAD by an additional factor of 4–5 in 2050 and 9–13 in 2100. Relatively, SLR and land subsidence are the main drivers of the increase in flood risk, followed by GDP growth (supplementary *Figure S6*).

The RCP8.5 high-end scenario of SLR, land subsidence, and economic growth leads to the highest simulated EAD, which can reach US$ 127 (41–409) billion/year, or 2.4% (0.8%–9.0%) of local GDP in 2100 (*Fig. 4*). Even under the optimistic emission scenario of RCP4.5, the EAD in 2100 could reach 0.8% (0.4%–1.4%) of local GDP, compared to the current value of 0.03%.

The current EAC is 2.4 persons per year, which is comparable with the officially reported annual casualties (1.6 persons/year) during 2000–2009 (Shanghai Bureau of Civil Affairs, 2014). Under a BAU trajectory, the simulated EAC increases by a factor of 7 (4–17) by 2050 and 84 (20–405) by 2100 compared with the current condition due to the combined influence of SLR, land subsidence, and population growth. Particularly, the EAC is projected to reach 18 (12–41) casualties/year in 2050 and 278 (94–978) casualties/year in 2100 under the RCP8.5 high-end scenario (supplementary *Figure S7*).

4.2. Reduction in economic damages by adaptation strategies

All adaptation strategies can effectively reduce the current EAD from US$ 106 million/year (BAU) to 0.04–33 million/year depending on the strategy (*Fig. 5*). The largest reductions in future EAD are accomplished by implementing the barrier and hybrid strategies.

4.2.1. Hard strategies

The barrier and floodwall strategies can significantly reduce the EAD for both current and future scenarios. Using a new storm-surge barrier with a 1000-year protection level designed for the RCP4.5 scenario (median estimate) for 2100, the barrier strategy reduces the current EAD from US$ 106 million/year to 0.2 million/year. In 2100, this strategy can still decrease the EAD by ≥97% from the BAU trajectory, maintaining the EAD/GDP ratios to ≤0.007% in all scenarios except in the 95%-bound estimate of RCP8.5 high-end scenario, which

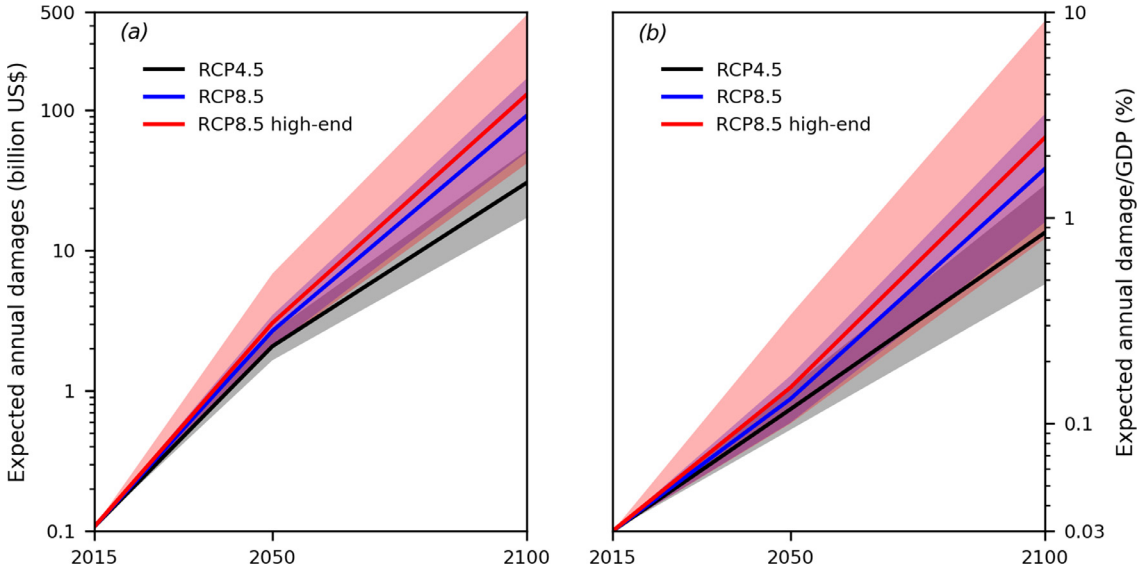

Fig. 4. Expected annual damages (a) and their ratios to local GDP (b) in a business-as-usual trajectory (median estimates with 5%–95% bounds).

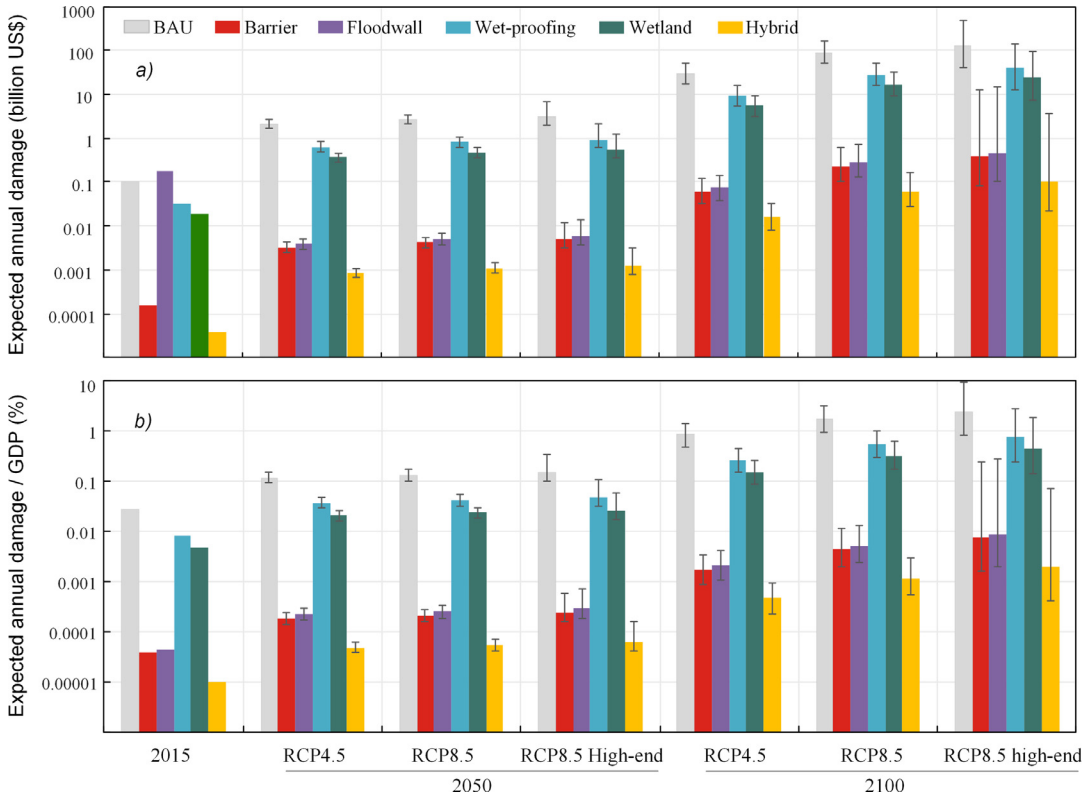

Fig. 5. Expected annual damages (a) and their ratios to GDP (b) with business-as-usual (BAU) trajectory and different adaptation strategies (median estimates with 5%–95% bounds).

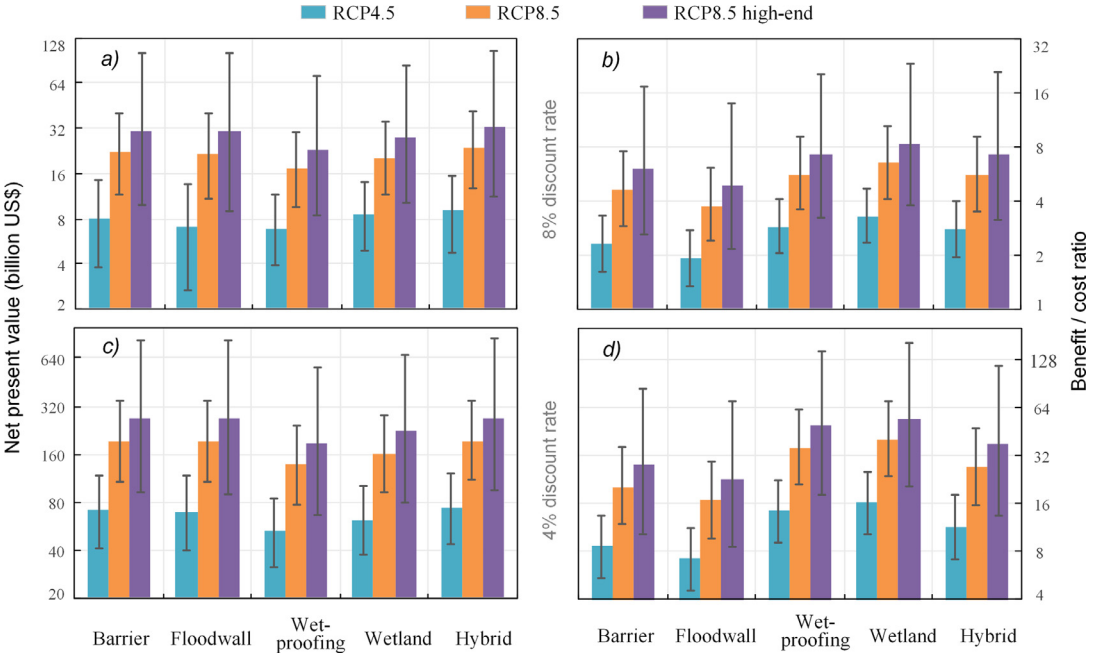

Fig. 6. The net present values (median estimates with 5%–95% bounds) of the adaptation strategies with discount rates of 8% (a) and 4% (c), and the respective benefit/cost ratios (b and d).

can see an EAD/GDP ratio of 0.24%. The floodwall strategy can also effectively reduce the EAD to a low level of US$ 0.2 million/year in 2015 and US$ 0.07 (0.04–0.1) – 0.5 (0.1–14.6) billion/year in 2100, making it slightly less effective than the barrier strategy.

4.2.2. Soft strategies

The wet-proofing strategy leads to a 69% reduction in the current EAD, from US$ 106 million/year to US$ 33 million/year. However, as the soft strategies cannot prevent rising seawaters from entering the city, their effectiveness is limited under future scenarios. Particularly for the RCP8.5 high-end scenario, the EAD with the wet-proofing strategy increases to US$ 0.9 (0.6–2.1) billion/year, or 0.05% (0.03%–0.1%) of local GDP, by 2050; this value further increases to US $ 39.8 (12.8–145.3) billion/year, or 0.8% (0.2%–2.8%) of local GDP, by

2100. The effectiveness can be greatly enhanced by coastal wetlands, which reduce the current EAD to US$ 19 million/year, or 0.005% of local GDP. However, the EAD/GDP ratio could reach 0.2% (0.09%–0.3%) – 0.5% (0.2%–2%) by 2100 under the RCP4.5 and RCP8.5 high-end scenarios, respectively, suggesting a reduction in the effectiveness of the soft strategies with SLR.

4.2.3. Hybrid strategy

The hybrid strategy can reduce the current EAD from US$ 106 million/year to 0.04 million/year. In 2100, the EAD under the hybrid strategy is US$ 0.02 (0.008–0.03) billion/year in the RCP4.5 scenario and US$ 0.1 (0.02–3.7) billion/year in the RCP8.5 high-end scenario. Specifically, all EAD values are less than 1% of the EAD under the BAU trajectory and only 26%–29% of the EAD under the barrier strategy. Even with the RCP8.5 high-end scenario, the EAD/GDP can be 0.002% (0.0004%–0.07%), dramatically lower than the value of 2.4% (0.8%–9.0%) under the BAU trajectory.

4.3. Cost-benefit analysis of adaptation strategies

Overall, the hard strategies (both barriers and floodwalls) have higher NPVs, while the soft strategies have higher benefit/cost ratios (*Fig. 6*). Among the two hard strategies, the barrier strategy has better performance in terms of both the benefit/cost ratio and the NPV. Among the soft strategies, the wetland strategy has a higher benefit/cost ratio and a higher NPV than the wet-proofing strategy. The barrier strategy has a NPV ranging from US$ 8.0 (3.7–14.3) billion under the RCP4.5 scenario to 31.2 (9.9–100.7) billion under the RCP8.5 high-end scenario, compared to the NPV of US$ 8.5 (4.9–13.9) – 27.7 (10.2–83.7) billion obtained by the wetland strategies. In contrast, the barrier strategy has benefit/cost ratios ranging from 2.3 (1.6–3.3) to 6.0 (2.6–17.0), lower than those of the wetland strategy ranging from 3.3 (2.3–4.1) to 8.4 (3.7–23.3).

The cumulative benefits can pay off the total costs (i.e., the initial investments and maintenance costs) much earlier using the soft strategies than using the hard strategies (*Fig. 7a*). The wetland strategy could obtain the earliest payoff year: 2035 (2032–2039) under the RCP4.5 scenario and 2031 (2025–2036) under the RCP8.5 high-end scenario. In contrast, the barrier strategy could obtain a later payoff year: 2045 (2038–2055) under the RCP4.5 scenario and 2036 (2038–2055) under the RCP8.5 high-end scenario.

The hybrid strategy combines the advantages of both the hard and the soft strategies. It has a benefit/cost ratio of 2.8 (1.9–4.0) – 7.2 (3.1–20.9), lying in between the values of the hard and soft strategies. Regarding the payoff period, the hybrid strategy also performs in between the hard and soft strategies: the cumulative benefits pay off the total costs by 2040 (2036–2047) and 2034 (2028–2041) under the RCP4.5 and RCP8.5 high-end scenarios, respectively. In terms of the NPV, the hybrid strategy performs better than all other strategies, with a value ranging from US$ 9.0 (4.8–15.4) billion under the RCP4.5 scenario to 32.3 (11.0–103.6) billion under the RCP8.5 high-end scenario.

We also assessed the economic performance of other building-code strategies, including elevation and dry-proofing. Across all scenarios, the benefit/cost ratios of the elevation strategy are >1 and slightly lower than that of the wet-proofing strategy. The dry-proofing strategy is the most expensive, with a discounted total cost of US$ 13.8 billion, and it yields a benefit/cost ratio <1 under the RCP4.5 scenario. However, its benefit/cost ratio reaches 1.3 and 1.7 in the RCP8.5 and RCP8.5 high-end scenarios, respectively.

4.4. Reduction in potential casualties by adaptation strategies

The EAC can be reduced by $>95\%$ using the hard and hybrid strategies and by $>73\%$ using the building elevation strategy (supplementary *Figure S8)*. The wet-proofing and dry-proofing strategies cannot directly reduce the EAC because they are applied only when the flood depth is low (≤ 2 m) that causes few casualties. However, the two strategies can still play a role in saving lives through mechanisms such as increasing risk awareness, which is not considered in this study.

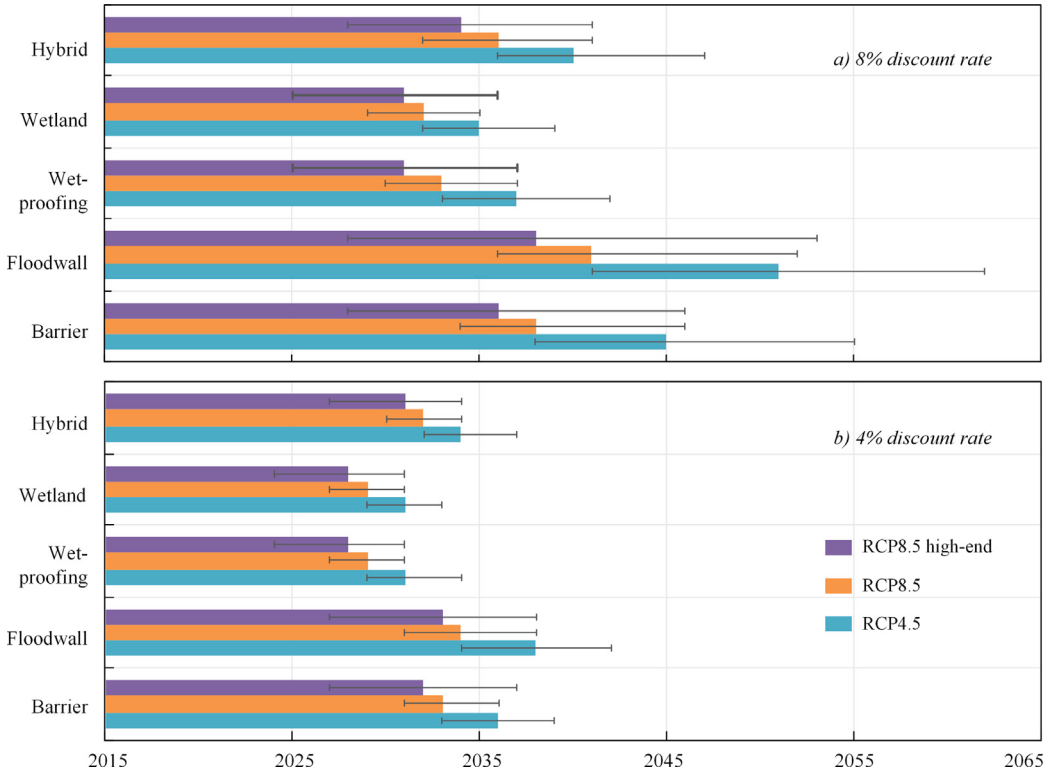

Fig. 7. The payoff year in which the cumulative benefits exceed the costs (median estimates with 5%–95% bounds).

Hence, all the strategies can be more welfare enhancing if the reduction in the EAC is included.

5. Discussion

5.1. Robust performance of adaptation strategies against uncertainties

We show that all adaptation strategies are economically attractive (benefit/cost ratios > 1), with the exception of the dry-proofing strategy under the RCP4.5 scenario with a high-bound discount rate of 8%. With lower discount rates, all strategies without exception become economically attractive under all scenarios, and the benefit/cost ratios of all strategies increases. With a 4% discount rate, the benefit/cost ratios increase to 2.1–162.3 (*Fig. 6d*), the NPVs increase to US$ 16.0–850.5 billion (*Fig. 6c*), and the payoff period is reached before 2024–2042 (*Fig. 7b*). Economic attractiveness is robust to a wide-range SLR estimate (5%–95% bounds). Across all scenarios, estimate bounds, and discount rates, the hybrid strategy outperforms the other strategies and has the highest NPVs and moderate benefit/cost ratios in between soft and hard strategies. In China, the official discount rate has decreased from 12% in the 1990 s to the current level of 8% (NDRC and MHURD, 2006) and is expected to decrease further with stabilizing GDP growth. Thus, our results suggest the adaptation strategies have a robust performance against uncertainties associated with discount rates.

The economic performance of the adaptation strategies should be higher if their benefit in terms of reducing indirect flood risk is considered. For example, in New York City (Aerts et al., 2014), the total damage (direct and indirect) can be 2.5 times the direct damage to buildings and vehicles. If such a scaling factor is applied in calculating the benefits, the benefit/cost ratios would be 2.5-fold higher than the presented values.

Nevertheless, this paper does not assess several uncertainties associated with: (1) flood frequency analysis (Botto et al., 2014); (2) compound conditions of storm surges, extreme precipitation, and upstream discharge (Ward et al., 2018); and (3) changing storm climatology (Lin et al., 2016). Moreover, city-level socioeconomic scenarios could be further elaborated, e.g., by considering the aging population and immigration policies in Shanghai (Gu et al., 2018). Future studies can improve the flood risk and cost-benefit analyses by accounting for a deeply uncertain future (Hu et al., 2019).

5.2. Policy implications and recommendations

Under current conditions, the simulated flood risk is already high in Shanghai. The EAD (direct damage to buildings and vehicles) is 150% higher in Shanghai than in New York (US$ ~71 million/year), while the EAD/GDP ratio is 5-fold higher in Shanghai than in New York (0.006%) (Aerts et al., 2014). Thus, flood risk adaptation strategies are urgently needed in Shanghai, even under current conditions. Shanghai is considered one of the best protected Chinese cities based on the 1000-year design standard of its floodwall. However, that standard is associated with the data up to 1984, while SLR and land subsidence have rapidly lowered the protection level in central Shanghai to a < 200-year level (Wang et al., 2012; Xian et al., 2018). Thus, immediate action is required, and this conclusion is supported by the positive NPV results associated with a high-bound discount rate of 8%.

Our analysis shows the importance of considering future SLR and land subsidence in designing the hard adaptation strategies. The future-minded design can reduce the EAD in 2100 to relatively low levels and enable these hard strategies, particularly the barrier strategy, to yield benefit/cost ratios >1. In contrast, a barrier built for the current conditions will result in the EAD/GDP ratio in 2100 ranging from 0.3% (0.2%–0.5%) under the RCP4.5 scenario to 1.0% (0.3%–6.6%) under the RCP 8.5 high-end scenario. This result shows that hard protection strategies designed for current conditions can lower current risk; however, without further strengthening to anticipate future SLR, they may lead to large-scale disasters in the coming decades if they are overtopped or breached. High reliability levels are difficult to obtain for hard protection strategies including storm surge barriers due to uncertainties of SLR and technical failure (Kwadijk et al., 2010). From cases in developed countries, an important lesson learned in relation to the design of future flood protection is to create flexible structures that allow for adjustments to climate change given the uncertainty of long-term SLR (Aerts and Botzen, 2012).

Compared with the hard strategies, the soft strategies have higher benefit/cost ratios. However, the soft strategies are less capable of reducing the future EAD. With the wetland strategy, the EAD/GDP ratio would reach 0.2% (0.09%–0.3%) – 0.5% (0.2%–2%) of local GDP in 2100 under the RCP4.5 and RCP8.5 high-end scenarios, respectively. The poor performance of the wetland strategy is mainly because the new designed wetland cannot shield the mouth of the Huangpu River, which runs through downtown Shanghai and has a tidal influence that cannot be prevented by the new wetland (*Fig. 1e*). Therefore, an economically attractive strategy may still perform poorly in terms of reducing the flood risk. Thus, the findings in this paper agree with the results of other studies (Hinkel et al., 2018; Jongman, 2018) and reveals that the soft strategies, while having high benefit/cost ratios, are not a one-size-fits-all solution to coastal flooding in a changing climate. Our findings also indicate that the performance of adaptation strategies should be interpreted in terms of both (1) the benefit/cost ratios of the adaptation investment and (2) the residual flood risk.

The current master plan of Shanghai (2017–2035) states that the city should upgrade its hard flood protection system (i.e., floodwalls, sea dikes, and barriers) to ensure flood adaptation to future SLR. Our study reveals that, although hard strategies can reduce the flood risk to a low level for both current and future conditions, the residual flood risk from using these strategies still needs to be addressed. Residual flood risk comes from extreme low-probability storm surges, such as that from Hurricane Sandy in New York in 2012, and from levee failure similar to that experienced by New Orleans during Hurricane Katrina in 2005. The residual risk can be further reduced by combining the barrier strategy with both the wet-proofing and the coastal wetland strategies to form a hybrid strategy. The hybrid strategy outperforms all other strategies in terms of benefit/cost ratios, NPVs, and EAD/GDP ratios across all 27 combinations of the three discount rates, three SLR scenarios, and three SLR estimate bounds. Therefore, soft measures, such as wet-proofing and coastal wetland development, can play a critical role in flood risk management, although on their own, they cannot maintain the future flood risk at a low level. Additionally, coastal wetlands can enhance social welfare by providing multiple ecosystem services, e.g., carbon sequestration, biodiversity, and aesthetic value (Hinkel et al., 2018).

A hybrid strategy is consistent with the flood risk management practices in Rotterdam, the Netherlands, where building codes and spatial planning play a critical role in forming a multilayered flood management system, including hard protection and evacuation-preparedness strategies (van Vliet and Aerts, 2015). However, the advantages of a hybrid strategy over other strategies should not be directly applied to other cases. The choice of adaptation strategy should depend on the local biophysical and socioeconomic environment. In the real world, the feasibility of flood adaptation measures depends on many factors, e.g., wealth and risk awareness of individuals, businesses, and government entities (Aerts et al., 2018; Hinkel et al., 2018). Based on an analysis of the social and economic feasibility of the adaptation measures, flexible adaptation pathways can be developed (Kwakkel et al., 2015). In China, both flood risk information and adaptation evaluations are rare in the literature (Du et al., 2019). Our methodology could help coastal cities evaluate their future flood risk and potential adaptation strategies.

6. Conclusion

This study presents an integrated modeling framework to simulate the nonstationarity of flood risk in Shanghai and to analyze the costs and benefits of adaptation strategies used to reduce flood risk. The results show that it is important for flood adaptation strategies to counteract the challenges generated from a changing socio-physical context. The current modeled flood risk (US$ 106 million/year, or 0.03% of the 2015 GDP) is already large in Shanghai, as SLR and land subsidence have already reduced flood protection levels and exacerbated the flood risk. SLR, land subsidence, and socioeconomic development will cause a sharp increase in the potential future flood risk: the EAD/GDP ratio may reach a level as high as 2.4% (0.8%–9.0%) by 2100 in a RCP8.5 high-end scenario. SLR and land subsidence are the main drivers of the increase in flood risk, followed by GDP growth.

Flood risk can be reduced significantly through hard protection strategies (e.g., storm-surge barriers). In comparison, soft strategies (e.g., wetlands) have higher benefit/cost ratios but result in a larger residual risk by 2100 . A hybrid strategy that combines the elements of hard strategies and soft strategies outperforms both single-strategy approaches in terms of lower future risk and higher benefit/cost ratios. The hybrid strategy can serve as a robust flood adaptation strategy for Shanghai. This finding is consistent with the findings of other studies (Aerts et al., 2014; Hinkel et al., 2018; Jongman, 2018). Clearly, managing flood risk requires a multi-scale approach, going beyond the use of single measures. The methodology developed in this paper can help to bring Shanghai and other coastal cities an economically and socially feasible adaptation strategy despite uncertainty in future conditions.

CRediT authorship contribution statement

Shiqiang Du: Methodology, Formal analysis, Visualization, Writing - review & editing. **Paolo Scussolini:** Conceptualization, Methodology, Writing - review & editing. **Philip J. Ward:** Conceptualization, Methodology, Writing - review & editing. **Min Zhang:** Software, Validation. **Jiahong Wen:** Software, Validation. **Luyang Wang:** Software, Validation. **Elco Koks:** Software, Validation. **Andres Diaz-Loaiza:** Software, Validation. **Jun Gao:** Investigation, Resources. **Qian Ke:** Investigation, Resources. **Jeroen C.J.H. Aerts:** Conceptualization, Methodology, Writing - review & editing.

Declaration of Competing Interest

The authors declare that there is no conflict of interest.

Acknowledgements

This research was funded by the National Natural Science Foundation of China (grant nos. 41871200, 41730642, 41701001, 51761135024) and the National Key Research and Development Program of China (2017YFC1503001). PJW, JCJHA, and PS received funding from the Netherlands Organization for Scientific Research (NWO) in the form of a VIDI grant (grant no. 016.161.324), a VICI grant (grant no 453.140.006), and a grant ALWOP.164, respectively. Mr. Xin Liu from Shanghai Xinyuan Engineering Cost Consulting Co., Ltd. helped to estimate the land-based maximum values, and the costs of the applied adaptation strategies.

Supplementary materials

Supplementary material associated with this article can be found, in the online version, at doi:10.1016/j.gloenvcha.2020.102037.

References

Aerts, J., Botzen, W.J.W., Emanuel, K., Lin, N., de Moel, H., Michel-Kerjan, E.O., 2014. Evaluating Flood Resilience Strategies for Coastal Megacities. Science 344, 472–474. https://doi.org/10.1126/science.1248222.

Aerts, J.C.J.H., Botzen, W.J., Clarke, K.C., Cutter, S.L., Hall, J.W., Merz, B., Michel-Kerjan, E., Mysiak, J., Surminski, S., Kunreuther, H., 2018. Integrating human behaviour dynamics into flood disaster risk assessment. Nat. Climate Change 8, 193–199. https://doi.org/10.1038/s41558-018-0085-1.

Aerts, J.C.J.H., Botzen, W.J.W., 2012. Climate adaptation cost for flood risk management in the Netherlands, Storm Surge Barriers to Protect New York City, pp. 99–113. 10.1061/9780784412527.007.

Balica, S.F., Wright, N.G., Meulen, F., 2012. A flood vulnerability index for coastal cities and its use in assessing climate change impacts. Nat. Hazards 64, 73–105. https://doi.org/10.1007/s11069-012-0234-1.

Benoit, M., Marcos, F., Becq, F., 1997. Development of a third generation shallow-water wave model with unstructured spatial meshing,. In: 25th International Conference on Coastal Engineering, Orlando, USA, pp. 465–478. https://doi.org/10.1061/9780784402429.037.

Botto, A., Ganora, D., Laio, F., Claps, P., 2014. Uncertainty compliant design flood estimation. Water Resour. Res. 50, 4242–4253. https://doi.org/10.1002/2013wr014981.

de Ruig, L.T., Barnard, P.L., Botzen, W.J.W., Grifman, P., Hart, J.F., de Moel, H., Sadrpour, N., Aerts, J.C.J.H., 2019. An economic evaluation of adaptation pathways in coastal mega cities: An illustration for Los Angeles. Sci. Total Environ. 678, 647–659. https://doi.org/10.1016/j.scitotenv.2019.04.308.

DHI MIKE, 2011. 1 D-2 D Modelling – user manual. DHI water & environment. http://manuals.mikepoweredbydhi.help/2017/Water_Resources/MIKE_FLOOD_UserManual.pdf.

Di Mauro, M., De Bruijn, K., 2012. Application and validation of mortality functions to assess the consequences of flooding to people. J. Flood Risk Manag. 5, 92–110. https://doi.org/10.1111/j.1753-318X.2011.01131.x.

Du, S., Cheng, X., Huang, Q., Chen, R., Ward, P.J., Aerts, J.C.J.H., 2019. Brief communication: Rethinking the 1998 China floods to prepare for a nonstationary future. Nat. Hazards Earth Syst. Sci. 19, 715–719. https://doi.org/10.5194/nhess-19-715-2019.

Du, S., Gu, H., Wen, J., Chen, K., Van Rompaey, A., 2015. Detecting flood variations in shanghai over 1949-2009 with Mann-Kendall tests and a newspaper-based database. Water 7, 1808–1824. https://doi.org/10.3390/w7051808.

Ehrlich, D., Melchiorri, M., Florczyk, A.J., Pesaresi, M., Kemper, T., Corbane, C., Freire, S., Schiavina, M., Siragusa, A., 2018. Remote sensing derived built-up area and population density to quantify global exposure to five natural hazards over time. Remote Sens. 10, 1378. https://doi.org/10.3390/rs10091378.

Environment Agency, 2012. TE2100 plan: managing flood risk through London and the Thames estuary. London, UK. https://assets.publishing.service.gov.uk/government/uploads/system/uploads/attachment_data/file/322061/LIT7540_43858f.pdf.

Gu, H., Du, S., Liao, B., Wen, J., Wang, C., Chen, R., Chen, B., 2018. A hierarchical pattern of urban social vulnerability in Shanghai, China and its implications for risk management. Sustain. Cities Soc. 41, 170–179. https://doi.org/10.1016/j.scs.2018.05.047.

Hallegatte, S., Green, C., Nicholls, R.J., Corfee-Morlot, J., 2013. Future flood losses in major coastal cities. Nat. Clim. Change 3, 802–806. https://doi.org/10.1038/nclimate1979.

Hervouet, J.M., 2000. TELEMAC modelling system: an overview. Hydrol. Process. 14, 2209–2210 10.1002/1099-1085(200009)14:13<2209::AID-HYP23>3.0.CO;2-6.

Hinkel, J., Aerts, J.C.J.H., Brown, S., Jiménez, J.A., Lincke, D., Nicholls, R.J., Scussolini, P., Sanchez-Arcilla, A., Vafeidis, A., Addo, K.A., 2018. The ability of societies to adapt to twenty-first-century sea-level rise. Nat. Clim. Change. https://doi.org/10.1038/s41558-018-0176-z.

Hu, H., Tian, Z., Sun, L., Wen, J., Liang, Z., Dong, G., Liu, J., 2019. Synthesized trade-off analysis of flood control solutions under future deep uncertainty: An application to the central business district of Shanghai. Water Res. 166, 115067. https://doi.org/10.1016/j.watres.2019.115067.

Jevrejeva, S., Grinsted, A., Moore, J.C., 2014. Upper limit for sea level projections by 2100. Environ. Res. Lett. 9, 104008. https://doi.org/10.1088/1748-9326/9/10/104008.

Jiang, T., Zhao, J., Chao, L., Wang, Y., Su, B., Jing, C., Wang, R., Gao, C., 2018. Projection of national and provincial economy under the shared socioeconomic pathways in China. Adv. Clim. Change Res. 1–10. https://doi.org/10.12006/j.issn.1673-1719.2017.161.

Jiang, T., Zhao, J., Jing, C., Chao, L., Wang, Y., Sun, H., Wang, A., Huang, J., Su, B., Wang, R., 2017. National and provincial population projected to 2100 under the shared socioeconomic pathways in China. Adv. Clim. Change Res. 1–12. https://doi.org/10.12006/j.issn.1673-1719.2016.249.

Jongman, B., 2018. Effective adaptation to rising flood risk. Nat. Commun. 9, 1986. https://doi.org/10.1038/s41467-018-04396-1.

Jonkman, S.N., Kok, M., Vrijling, J.K., 2008. Flood risk assessment in the Netherlands: a case study for dike ring south Holland. Risk Anal. 28, 1357–1374. https://doi.org/10.1111/j.1539-6924.2008.01103.x.

Ke, Q., 2014. Flood Risk Analysis for Metropolitan Areas –A Case Study for Shanghai. DelftUniversity of Technology, Delft, The Netherlands, p. 193. 10.4233/uuid:61986b2d-72de-45e7-8f2a-bd61c725325d.

Koks, E.E., 2019. DamageScanner: Python tool for disaster damage assessments (Version v0.2.1). 10.5281/zenodo.2551016.

Kreibich, H., Christenberger, S., Schwarze, R., 2011. Economic motivation of households to undertake private precautionary measures against floods. Nat. Hazards Earth Syst.

Sci. 11, 309–321. https://doi.org/10.5194/nhess-11-309-2011.
Kwadijk, J.C.J., Haasnoot, M., Mulder, J.P.M., Hoogvliet, M.M.C., Jeuken, A.B.M., van der Krogt, R.A.A., van Oostrom, N.G.C., Schelfhout, H.A., van Velzen, E.H., van Waveren, H., de Wit, M.J.M., 2010. Using adaptation tipping points to prepare for climate change and sea level rise: a case study in the Netherlands. Wires Clim. Change 1, 729–740. https://doi.org/10.1002/wcc.64.
Kwakkel, J.H., Haasnoot, M., Walker, W.E., 2015. Developing dynamic adaptive policy pathways: a computer-assisted approach for developing adaptive strategies for a deeply uncertain world. Clim. Change 132, 373–386. https://doi.org/10.1007/s10584-014-1210-4.
Lasage, R., Veldkamp, T.I.E., de Moel, H., Van, T.C., Phi, H.L., Vellinga, P., Aerts, J.C.J.H., 2014. Assessment of the effectiveness of flood adaptation strategies for HCMC. Nat. Hazards Earth Syst. Sci. 14, 1441–1457. https://doi.org/10.5194/nhess-14-1441-2014.
Lin, N., Kopp, R.E., Horton, B.P., Donnelly, J.P., 2016. Hurricane Sandy's flood frequency increasing from year 1800 to 2100. Proc. Natl. Acad. Sci., 201604386. https://doi.org/10.1073/pnas.1604386113.
Lu, Y., 2007. Approaching strategy and countermeasures to denfend against typhoon in Shanghai (in Chinese). Urban Roads Bridges & Flood Control, 29-33+12. 10.3969/j.issn.1009-7716.2007.04.010.
Ma, Z., Li, B., Zhao, B., Jing, K., Tang, S., Chen, J., 2004. Are Artificial Wetlands Good Alternatives to Natural Wetlands for Waterbirds?–A Case Study on Chongming Island 13. Biodiversity & Conservation, China, pp. 333–350. https://doi.org/10.1023/B:BIOC.0000006502.96131.59.
Martínez-Gomariz, E., Gómez, M., Russo, B., Sánchez, P., Montes, J.-A., 2018. Methodology for the damage assessment of vehicles exposed to flooding in urban areas. J. Flood Risk Manag. 0, e12475. https://doi.org/10.1111/jfr3.12475.
Najibi, N., Devineni, N., 2018. Recent trends in the frequency and duration of global floods. Earth Syst. Dynam. 9, 757–783. https://doi.org/10.5194/esd-9-757-2018.
NDRC and MHURD, 2006. Construction Projects Economic Evaluation: Method and Parameter. Planning Press of China, Beijing, China.
O'Neill, B.C., Kriegler, E., Riahi, K., Ebi, K.L., Hallegatte, S., Carter, T.R., Mathur, R., van Vuuren, D.P., 2014. A new scenario framework for climate change research: the concept of shared socioeconomic pathways. Clim. Change 122, 387–400. https://doi.org/10.1007/s10584-013-0905-2.
Scussolini, P., Tran, T.V.T., Koks, E., Diaz-Loaiza, A., Ho, P.L., Lasage, R., 2017. Adaptation to sea level rise: a multidisciplinary analysis for Ho Chi Minh City, Vietnam. Water Resour. Res. 53, 10841–10857. https://doi.org/10.1002/2017WR021344.
Sengupta, D., Chen, R., Meadows, M.E., 2018. Building beyond land: An overview of coastal land reclamation in 16 global megacities. Appl. Geogr. 90, 229–238. https://doi.org/10.1016/j.apgeog.2017.12.015.
Shanghai Bureau of Civil Affairs, 2014. Yearbook of natural disaster response in Shanghai in 2013 (inner report). Shanghai, China.
Shanghai Municipal People's Government, 2018. Shanghai Master Plan (2017-2035) (in Chinese). Shanghai Urban Planning and Land Resource Administration Bureau, Shanghai. http://www.shanghai.gov.cn/newshanghai/xxgkfj/2035004.pdf.
Shanghai Statistical Bureau, 2016. Shanghai Statistical Yearbook 2016. China Statistical Press, Beijing. http://tjj.sh.gov.cn/tjnj/sh2017e.htm.
Shen, J., Du, S., Huang, Q., Yin, J., Zhang, M., Wen, J., Gao, J., 2019. Mapping the city-scale supply and demand of ecosystem flood regulation services – A case study in Shanghai. Ecol. Indic. 106, 105544. https://doi.org/10.1016/j.ecolind.2019.105544.
SMWA, 2013. Shanghai plan for sea dikes (2011-2020). Shanghai, China.
Thieken, A.H., Cammerer, H., Dobler, C., Lammel, J., Schöberl, F., 2016. Estimating Changes in Flood Risks and Benefits of Non-Structural Adaptation Strategies – A Case Study from Tyrol 21. Mitig Adapt Strateg Glob Change, Austria, pp. 343–376. https://doi.org/10.1007/s11027-014-9602-3.
van Vliet, M., Aerts, J.C.J.H., 2015. Adapting to Climate Change in Urban Water Management: Flood Management in the Rotterdam–Rijnmond Area. In: Grafton, Q., Daniell, K.A., Nauges, C., Rinaudo, J.-D., Chan, N.W.W. (Eds.), Understanding and Managing Urban Water in Transition. Springer, Netherlands, pp. 549–574. https://doi.org/10.1007/978-94-017-9801-3_25. Dordrecht.
Wahl, T., Haigh, I.D., Nicholls, R.J., Arns, A., Dangendorf, S., Hinkel, J., Slangen, A.B.A., 2017. Understanding extreme sea levels for broad-scale coastal impact and adaptation analysis. Nat. Commun. 8, 16075. https://doi.org/10.1038/ncomms16075.
Wallemacq, P., Below, R., McLean, D., 2018. Economic Losses, Poverty & Disasters (1998-2017). Centre for Research on the Epidemiology of Disasters (CRED). UN Office for Disaster Risk Reduction (UNISDR), Brussels, BELGIUM. https://www.unisdr.org/we/inform/publications/61119.
Wang, J., Gao, W., Xu, S., Yu, L., 2012. Evaluation of the combined risk of sea level rise, land subsidence, and storm surges on the coastal areas of Shanghai. China. Clim. Change 115, 537–558. https://doi.org/10.1007/s10584-012-0468-7.
Wang, L.Y., Zhang, M., Wen, J.H., Chong, Z.T., Ye, Q.H., Ke, Q., 2019. Simulation of extreme compound coastal flooding in Shanghai (in Chinese). Adv. Water Sci. 30, 546–555. http://skxjz.nhri.cn/EN/Y2019/V30/I4/546.
Ward, P.J., Couasnon, A., Eilander, D., Haigh, I.D., Hendry, A., Muis, S., Veldkamp, T.I.E., Winsemius, H.C., Wahl, T., 2018. Dependence between high sea-level and high river discharge increases flood hazard in global deltas and estuaries. Environ. Res. Lett. 13, 084012. https://doi.org/10.1088/1748-9326/aad400.
Ward, P.J., de Moel, H., Aerts, J.C.J.H., 2011a. How are flood risk estimates affected by the choice of return-periods? Nat. Hazard Earth Sys. 11, 3181–3195. https://doi.org/10.5194/nhess-11-3181-2011.
Ward, P.J., Marfai, M.A., Yulianto, F., Hizbaron, D.R., Aerts, J.C.J.H., 2011b. Coastal inundation and damage exposure estimation: a case study for Jakarta. Nat. Hazards 56, 899–916. https://doi.org/10.1007/s11069-010-9599-1.
Wen, K., 2006. Meteorological Disasters in China (in Chinese). China Meteorological Press, Beijing, China.
Willner, S.N., Otto, C., Levermann, A., 2018. Global economic response to river floods. Nat. Clim. Change 8, 594–598. https://doi.org/10.1038/s41558-018-0173-2.
Winsemius, H.C., Aerts, J.C.J.H., van Beek, L.P.H., Bierkens, M.F.P., Bouwman, A., Jongman, B., Kwadijk, J.C.J., Ligtvoet, W., Lucas, P.L., van Vuuren, D.P., Ward, P.J., 2016. Global drivers of future river flood risk. Nat. Clim. Change 6, 381–385. https://doi.org/10.1038/nclimate2893.
Xian, S., Yin, J., Lin, N., Oppenheimer, M., 2018. Influence of risk factors and past events on flood resilience in coastal megacities: comparative analysis of NYC and Shanghai. Sci. Total Environ. 610, 1251–1261. https://doi.org/10.1016/j.scitotenv.2017.07.229.
Yin, J., Yin, Z.E., Yu, D.P., Xu, X.Y., 2012. Vulnerability analysis for storm induced flood: a case study of Huangpu river basin (in Chinese). Sci. Geogr. Sinica 32, 1155–1160. http://geoscien.neigae.ac.cn/CN/Y2012/V32/I9/1155.
Yin, J., Yu, D., Yin, Z., Wang, J., Xu, S., 2015. Modelling the anthropogenic impacts on fluvial flood risks in a coastal mega-city: A scenario-based case study in Shanghai. China Landsc. Urban Plan 136, 144–155. https://doi.org/10.1016/j.landurbplan.2014.12.009.
Zhang, M., Townend, I., Cai, H., He, J., Mei, X., 2018. The influence of seasonal climate on the morphology of the mouth-bar in the Yangtze Estuary. China Cont. Shelf Res. 153, 30–49. https://doi.org/10.1016/j.csr.2017.12.004.